Comparative Study of the Effect of Halloysite Nanocontainers on Autonomic Corrosion Protection of Polyepoxy Coatings on Steel by Salt-Spray Tests

Elena Shchukina,[1] Dmitry Grigoriev,[2] Tatyana Sviridova,[3] Dmitry Shchukin[1*]

[1]Stephenson Institute for Renewable Energy, University of Liverpool, L69 7ZF, Liverpool, UK. E-mail: d.shchukin@liverpool.ac.uk.

[2]Current affiliation: Fraunhofer Institute for Applied Polymer Research IAP, Geiselbergstraße 69, 14476 Potsdam-Golm, Germany.

[3]Belarusian State University, Faculty of Chemistry, 4 Nezavisimosti Av., 220030 Minsk, Belarus.

Abstract.

The comparative study was carried out to show the effect of the halloysite nanotubes loaded with three inhibitors with different properties (Korantin SMK, Halox 520 and $(NH_4)_2TiF_6$) as an additive for autonomic corrosion protection of polyepoxy coating on steel substrate. The comparison was carried out employing neutral salt-spray test (5 % NaCl, 35℃, different time). Commercial polyepoxy coating containing 20 wt% of zinc phosphate was used as a benchmark during testing. We demonstrated that inhibitor-loaded halloysites at 5 wt% concentration are able to successfully substitute 20 wt% zinc phosphate in the commercial polyepoxy coating even improving its corrosion protection performance, which depends in a large extend on the release profiles of the inhibitors loaded into halloysite nanotubes. On the contrary, addition of the free inhibitors into the coating showed complete deterioration of the corrosion protection properties for all inhibitors.

Key words.

Nanocontainer; Polymer coating; Autonomic protection; Halloysite.

Highlights

1. 1 wt% of the encapsulated inhibitor Korantin SMK has the efficiency of 20% Zn phosphate.
2. Controlled release of encapsulated corrosion inhibitors at different pH.
3. Corrosion protection of nanocontainer-impregnated coatings over 1000 h of salt spray test.

Introduction.

Recent achievements in nanocontainer-based autonomic corrosion protection coatings demonstrated high potential of inhibitor-loaded containers to attain autonomous effect to the standard coating formulations [1]. In general, nanocontainers' formation and loading in the size range of 20 nm to 50 μm require the ability to form a nanocontainer shell which should be stable, permeable to release/upload of the materials and possess other desired functionalities (magnetic, catalytic, conductive, targeting, etc.). In order to develop functionalized micro- and nanocontainers, one has to combine different properties in the shell structure and composition. There are several approaches demonstrated so far for the design of nanocontainer depot systems: (i) polymer containers [2], (ii) halloysites [3], (iii) nanocontainers with polyelectrolyte shell [4], (iv) layered double hydroxides [5] and, finally, (v) mesoporous inorganic materials [6]. Paper of Jadhav et al. [7] describing the use of the encapsulated linseed oil for self-healing coatings made this inhibitor as an environmentally friendly active cargo. Core–shell microcapsules of urea-resorcinol-formaldehyde shell and linseed oil core material were prepared for self-healing coatings [8]. The capsules contained linseed oil as an active material where Co-octoate as drier material and/or octadecylamine as corrosion inhibitor can be dissolved as additional function component. Other authors showed similar effects for polyurethane capsules with linseed oil core containing second corrosion inhibitor mercaptobenzothiazole [9]. Smart dual inhibiting effect was also observed for microcapsules containing Tung oil as a core and poly(styrene sulfonate)/poly(ethylene imine) multilayer shell with corrosion inhibitor benzotriazole intercalated within the shell [10]. Corrosion process changes pH in the local area releasing entrapped inhibitors and passivating corrosion area. Example of the Layer-by-Layer assembly (LbL) technology applied for formation of the inhibitor-loaded capsules is the encapsulation of 2-methylbenzothiazole and 2-mercaptobenzothiazole inside poly(styrene sulfonate)/poly (diallyldimethylammonium chloride) shell sensitive to the local pH changes [11]. These nanocapsules are compatible with epoxy coatings and stable during the mixing, application and curing processes. Carneiro et al. [12] showed double-loaded nanocontainers based not on the organic core – polyelectrolyte shell combination but on inorganic core (layered double hydroxides) containing 2-mercaptobenzothiazole inhibitor and poly(styrene sulfonate)/poly(allylamine

hydrochloride) polyelectrolyte shell loaded with Ce^{3+}. Release of the 2-mercaptobenzothiazole is based on the intrinsic properties of layered double hydroxides to intercalate ion-exchange species between layers while Ce^{3+} is electrostatically released by changing pH of polyelectrolyte shell.

Changes in the local environment of a coating during corrosion are mostly of chemical nature (*e.g.*, electrochemical potential, pH, ionic strength or humidity) which can trigger swelling/shrinkage of the nanocontainers or change permeability of the nanocontainer shells [13,14,15]. Utilizing pH shift as stimulus for corrosion inhibitor release is the most promising way to design autonomic coatings due to the local pH decrease in anodic areas and local pH increase in the cathodic ones [16]. There are several comprehensive reviews published so far describing various combinations of nanocontainers and inhibitors, nature of nanocontainers, release profiles and electrochemical studies of corrosion protection performance. H. Wei et *al.*, M.L. Zheludkevich et *al.* [17,18] surveyed anticorrosion performance of inhibitor-filled polymeric nano and microcontainers, halloysites, ion exchange clays and mesoporous silica capsules. Very detailed review by M.F. Montemor [19] summarized information about nano and microcontainers performance in the coatings acquired by localized techniques (scanning vibration electrode technique, SVET and scanning ion-selective electrode technique, SIET). Y. Lvov et al. [20,21,22] demonstrated halloysite nanotubes loaded with corrosion inhibitors benzotriazole, 2-mercaptobenzimidazole and 2-mercaptobenzothiazole as effective additives for autonomic protection coatings for copper protection. The authors used optical and SEM visualisation to confirm autonomic action of the halloysite additives after exposure to 0.5 M aqueous NaCl. Another paper of these authors [23] employed SVET to demonstrate protection properties on the micron scale on the artificial cracks in NaCl solution. SVET and electrochemical impedance spectroscopy (EIS) were also used by us for demonstration of the self-controlled inhibitor release properties of benzotriazole-loaded halloysites in sol-gel coatings for aluminium protection [3,24].

Despite large number of the papers devoted to the nanocontainer-based autonomic protection coatings, most of them use lab-scale analytical methods for characterisation of their performance: EIS, polarisation, SVET and various adapted electrochemical techniques. Only paper of M.L. Zheludkevich et *al.* [25] analysed the efficiency of the nanocontainer-based autonomic coatings using industrial methods. However, the

current numbers of the reported successful laboratory studies call for the transfer of the results to the industry for further commercialisation.

Here, we present comparative analysis of the halloysite nanocontainers loaded with three different inhibitors (Halox 520, Korantin SMK and $(NH_4)_2TiF_6$) as active ingredients for polyepoxy-based autonomic corrosion protection coatings. Anticorrosion performance was tested by neutral salt-spray test (ISO 9227, 5 wt% NaCl, 35℃, different time) and a standard commerci al polyepoxy paint (Lankwitzer-Lackfabric GmbH) containing 20 wt% of zinc phosphate was taken as a benchmark. Coating adhesion properties and comparative EIS date for the coatings with and without inhibitor-loaded nanocontainers are presented in Supporting Information section of the paper.

Experimental.

Materials

Corrosion inhibitors Korantin SMK (alkylphosphoric ester with the chain length of alkyls in the ester group ranging from C6 to C10) and Halox 520 (60 wt% solution of poly(3-ammoniumpropylethoxysiloxane)dodecanoate in ethanol) were provided by BASF company, Germany and C.H. Erbslöh GmbH & Co. KG, Germany, respectively. $(NH_4)_2TiF_6$ and sodium poly(methacrylate) (PMA) were purchased from Sigma-Aldrich and used without further purification. Halloysites were provided by Atlas Mining Company (Dragon Mine deposit, Utah, USA).

Preparation of nanocontainers

Halloysites are naturally occurring layered kaolin-like aluminosilicates with hollow tubular structure. The aluminum hydroxide and the silicon oxide layers are bond covalently with each other. The bilayer rolls up to a tube, i.e. a hollow cylinder with aluminum inside and silicon outside. Halloysite nanotubes used in the paper have inner lumen with diameter 15-20 nm with outer diameter around 50 nm (Figure 1a,b) and a specific surface area of 60 m^2/g with pore volume of 0.2 cm^3/g. Loading of the halloysite nanotubes with inhibitors was performed from the corresponding solutions under reduced pressure. 50 ml of 20 wt% ethanolic (Halox 520, Korantin SMK) or aqueous inhibitor solution ($(NH_4)_2TiF_6$) were mixed with 5 g of empty halloysites and then introduced into a desiccator with a reduced pressure. The air goes out from the halloysite inner volume, and is replaced by the solution containing corrosion inhibitor. The loading was performed three times followed by centrifugation in water at 5000

rpm. The inhibitor loading inside halloysite nanotubes was 20±1 wt% for all inhibitors presented in this work (measured by TGA, Linseis STA PT1000 with a heating rate 5 K/min under air), which is the maximal loading capacity for the natural halloysites of this type. Outer PMA polyelectrolyte layer was deposited onto inhibitor-loaded halloysites by electrostatic adsorption from the 5 wt% aqueous solution. 5 g of loaded halloysite nanotubes were added to the polyelectrolyte solution and incubated for 20 min. Then, the separation of the nanocontainers from the rest of polyelectrolyte solution was done by filtration followed by washing in water.

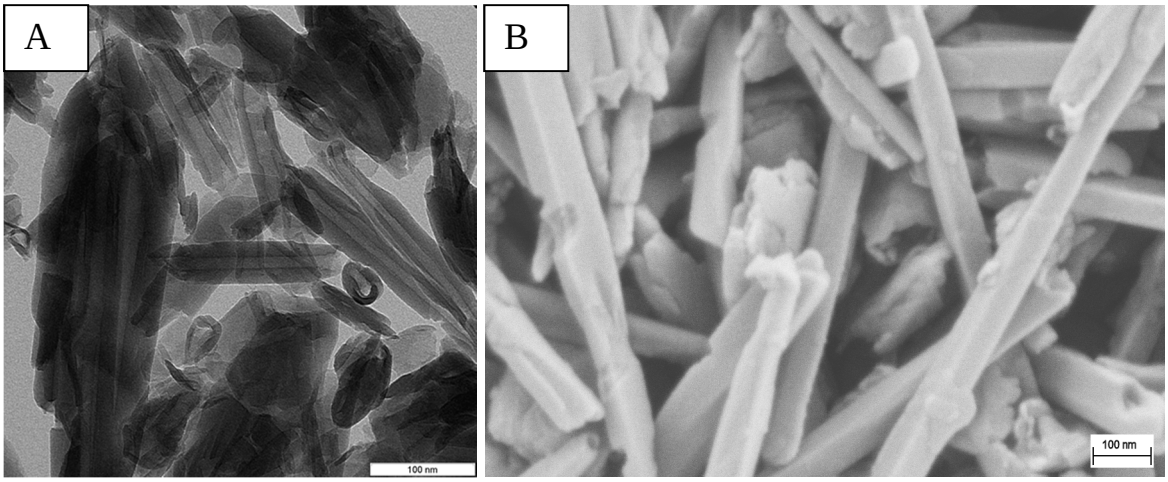

Figure 1. TEM (A) and SEM (B) of the halloysite nanotubes used as host containers for corrosion inhibitors. Scale bar is 100 nm.

Release measurements in aqueous media

The release kinetics of inhibitors encapsulated into halloysites was carried out in 5 % aqueous halloysite suspensions with various pH values mimicking the local pH changes which can be caused by the corrosion onset. The suspensions (500 ml each) were exposed to moderate continuous stirring (300 rpm) and pH was adjusted by HCl or NaOH. After defined time intervals, the suspensions aliquots of 2 ml were withdrawn in triplicate and replaced with the same aqueous solution. The collected samples were centrifuged at 5000 rpm to separate the supernatant from the dispersed halloysites. The supernatant was then analyzed by inductively coupled plasma atomic emission spectroscopy (ICP-AES, Shimadzu ICPE-9800, Japan) for detection of the signals from the elements unique for each inhibitor (P for Korantin SMK, Si for Halox 520 and Ti for $(NH_4)_2TiF_6$). The intensity values were used for the evaluation of inhibitor concentrations in the release medium and calculation of their release ratio.

Coating application

Inhibitor-loaded halloysites were added to the polyepoxy coating from Lankwitzer-Lackfabric GmbH at 1, 3 and 5 wt% concentration (which corresponds to 0.2 wt%, 0.6 wt% and 1 wt% of the inhibitor in the coating) by mixing with Ultra-Turrax high-speed homogenizer (IKA Werke, Staufen, Germany) at 2000 rpm stirring until the entire mixture became well-homogenized. This waterborne two component epoxy coating is a classical one with epoxy-rich binding agent making the basis for the parent lacquer (first component) and a typical water based amino-hardener (second component). Then, the coating was applied by spraying (spray-gun nozzle diameter 1.5 mm and processing pressure 4.5 bars) on the sand-cleaned steel plates. The plates were purchased from Q-Panel R-35 (Q-Lab, USA) with dimension (TxWxL) of 0.8x76x127 mm. The thickness of all deposited samples was in the range of 75-90 µm depending on the sample and quantity of the halloysites in the coating. We did not observe any leakage of the inhibitor from the halloysite nanotubes during coating application. According to our previous studies, halloysite nanotubes are homogeneously distributed in the coating matrix [3, 26]. The same polyepoxy paint both with 20 wt% of zinc phosphate and without zinc phosphate was deposited in a similar way for comparison. After application, the freshly coated panels were left for room temperature curing process for 7 days.

Characterisation

SEM measurements were carried out using a Gemini Leo 1550 instrument at an operation voltage of 3 keV. The samples were prepared by placing container aqueous suspension onto a glass substrate, drying and subsequent gold sputtering. Transmission electron microscopy was performed using Zeiss EM 912 Omega transmission electron microscope to analyze the structure of halloysite nanocontainers.

The coating thickness was measured with a coating thickness gauge, Surfix® Pro S, from PHYNIX, Germany. Anticorrosion performance was tested by neutral salt-spray test (Ascott CC450XP salt spray chamber, ISO 9227). Before testing in the salt spray chamber, the cured panels were handled as follows: the cut edges and back surface were protected using a transparent Scotch tape. Then, in the middle part of each panel a vertical scribe with the length of 7 cm and 1 mm width was made using the scribing

knife. The scribed panels were placed on the special racks in the salt spray chamber with the total inner volume of 450 L and conditions leading to the accelerated onset of corrosion: 100% rh, T = 35°C, continuous spraying of 5 wt% aqueous NaCl solution. The duration of NSS test was set to 500 h and 1000 h. Three parallel samples were measured to collect delamination statistics. The delaminated coatings were mechanically detached from rinsed and dried samples after salt spray test with the knife according to the DIN EN ISO 4628-8. The photographs of defected plates were digitised and transformed to the binary form. The total amount of pixels in corroded area was counted and divided by the length of the scribe. Finally, the backward transformation yielded the averaged value of the delamination independent of the specific measuring point across the scribe.

Results&Discussion.

The effect of the inhibitor-loaded halloysites inside the coatings is based on the controlled release of the corrosion inhibitor from halloysite nanotubes inside the damaged area of the coatings. The inhibitor releases in the damaged area from the neighbouring halloysite nanotubes and chemisorbs terminating corrosion. It is important to achieve high release rates of the encapsulated inhibitor both in acidic and in alkaline media for efficient protection effect because of the local pH changes caused by corrosion process [16].

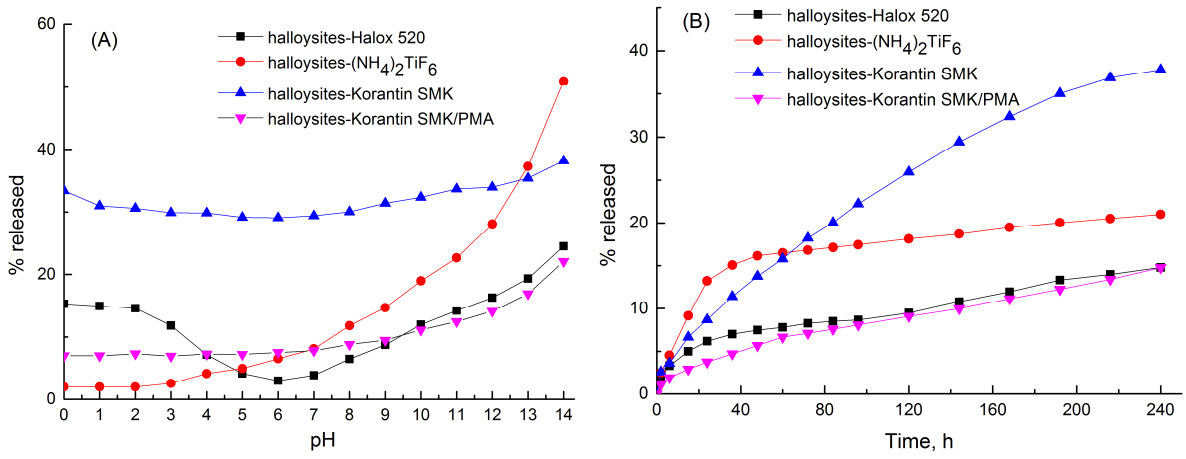

Figure 2. (A) – Release of the encapsulated corrosion inhibitors at different pH values after 168 hours of incubation for the studied halloysite-inhibitor combinations. (B) – Time-dependent release profiles of the encapsulated corrosion inhibitors at pH=10 for the studied halloysite-inhibitor combinations.

The nature of the encapsulated inhibitor has considerable influence on its release from the halloysite nanotubes at different pH values. As shown in Figure 2a, charged $(NH_4)_2TiF_6$ stays inside halloysite nanotubes at low pH values and then has a rapid release growth when pH increasing. This can be explained by the internal structure of the halloysite lumen consisting of gibbsite octahedral sheet (Al-OH) groups, which are positively charged at pH below 8 while the external surface is composed of the negatively charged siloxane groups (Si-O-Si) [27]. Similar effect was also observed for Halox 520. Its dodecanoate group is uncharged till pH around 5 (pK_a of n-dodecanoic acid is 5.3) which results in pronounced release from the halloysite nanotubes at low pH followed by decreasing to pH 7-8. Then, the release rate is rapidly increased due to the recharge of the inner halloysite lumen to the negative value and repulsion of the inhibitor out of it.

Another behaviour can be seen for the neutral Korantin SMK. This inhibitor has similar release rate almost within the whole pH range. Slight reduction is found at pH 5-7 with further increase above pH 12. Overall, the release efficiency for neutral Korantin SMK is higher than that of other inhibitors between pH 0 and 12 probably due to the absence of the electrostatic interactions with the inner lumen of the halloysite host. Addition of the PMA layer on the Korantin-loaded halloysites significantly reduces release, which can be caused by the additional PMA diffusion barrier at the nanotube ends.

Kinetic release curves at pH=10 (Fig. 2b) confirm the main conclusions derived from the pH-dependence of the inhibitor release (Fig. 2a). Charged corrosion inhibitors (Halox 520 and $(NH_4)_2TiF_6$) exhibit rapid initial release from negatively charged halloysite lumen achieving a saturation limit at around 80 hours of incubation. Neutral Korantin, on the contrary, shows gradual increase of the release with the time reaching saturation after more than 240 hours.

Application of the paint was done by spraying gun at various application times in order to achieve thickness of the dried coating compatible for all samples. No leakage of the corrosion inhibitor was observed from the intact coatings. Thicknesses of the dried coatings are tabulated in Table 1 after measurements of three parallel samples. No considerable effects of the loaded halloysites on the adhesion properties of the coating to steel substrate was observed (see Supporting Information, Figure S1).

Table 1. Thicknesses of the dried coatings on steel substrate.

Coating type	*Thickness, μm*
Standard coating with Zn phosphate	85±8
Standard coating without Zn phosphate	82±7
Standard coating with pure halloysites, 5 wt%	73±8
Standard coating with pure $(NH_4)_2TiF_6$, 5 wt% of inhibitor	72±9
Standard coating with pure Korantin SMK, 5 wt% of inhibitor	80±4
Standard coating with Halox 520 loaded halloysites, 5 wt%	81±7
Standard coating with $(NH_4)_2TiF_6$ loaded halloysites, 5 wt%	83±3
Standard coating with Korantin SMK loaded halloysites, 5 wt%	83±4
Standard coating with Korantin SMK loaded halloysites and PMA polyelectrolyte shell, 5 wt%	86±5
Standard coating with Korantin SMK loaded halloysites and PMA polyelectrolyte shell, 3 wt%	89±4
Standard coating with Korantin SMK loaded halloysites and PMA polyelectrolyte shell, 1 wt%	86±3

First, neutral salt spray tests of the standard polyepoxy coating both with 20 wt% zinc phosphate and without Zn phosphate were performed as a benchmark (Fig. 3) for 500 and 1000 h of test duration.

A B C D

Figure 3. Neutral salt spray test results for standard commercial polyepoxy coating with 20 wt% of Zn phosphate (A, delamination 1.4 mm), (B, delamination 3.2 mm) and without (C, delamination 3.7 mm, D, delamination 5.8 mm) after 500 h (A, C) and 1000 h (B, D). Plate size is 0.8x76x127 mm.

As one can see, complete removal of the zinc phosphate from the coating considerably increases coating's corrosion and degradation. There is corrosion propagation under the coating from artificial scribe and also signs of the blistering corrosion accompanied by delamination increase from 3.2 mm for Zn phosphate containing coating to 5.8 mm for the coating without Zn phosphate (after 1000 h of salt spray test). Direct addition of the inhibitors or pure halloysites in 5 wt% concentration to the polyepoxy coating without Zn phosphate did not improve corrosion protection performance (Figure 4).

(A) (B) (C)

Figure 4. Neutral salt spray test results for polyepoxy coating without Zn phosphate in the presence of 5 wt% of pure halloysite nanotubes (A, delamination 3.2 mm), Korantin SMK (B) and $(NH)_4TiF_6$ (C) corrosion inhibitors in pure form, 500 hours. Plate size is 0.8x76x127 mm.

Addition of pure, un-loaded halloysite nanoparticles did not make considerable changes in corrosion protection (Fig. 4a) resulting in 3.2 mm delamination, which is comparative to the coating without Zn phosphate (delamination 3.2 mm). However, addition of the pure corrosion inhibitors drastically decreased corrosion protection of the coatings, and after 500 h of salt spray test all exposed coating area was completely corroded (Figs. 4b,c). The possible explanation of this effect is the direct interaction between coating matrix and corrosion inhibitors which leads to the decrease of the barrier properties of the coating and termination of the inhibitor performance [6]. Proper use of the nanocontainers should isolate corrosion inhibitor from the coating providing its controlled release only in defected areas exposed to corrosion.

(A) (B) (C)

Figure 5. Neutral salt spray test results (1000 hours) for polyepoxy coating without Zn phosphate in the presence of Halox 520 loaded halloysite nanotubes, 5 wt% (A, delamination 2.2 mm); $(NH_4)_2TiF_6$ loaded halloysite nanotubes (B. delamination 3.4 mm); Korantin SMK loaded halloysite nanotubes (C, delamination 1.2 mm).

Encapsulation of the corrosion inhibitors into the halloysite nanotubes resulted in the increase of the protection efficiency (Fig. 5). The protection effect is well correlated to the release performance of the inhibitors from halloysite lumen (Fig. 2). Neutral inhibitors have the ability to be released at the triggered pH range sustainably. The small addition of the encapsulated Korantin SMK (1 wt% of the encapsulated inhibitor in the coating) achieved the efficiency of the 20 % Zn phosphate pigment in the coating. The isolation of the inhibitor followed by controlled release avoids the interaction between inhibitor and other components of the coating formulation resulting in more efficient use of the inhibiting agent. These findings are in the agreement with the EIS results for the standard commercial polyepoxy paint which demonstrated no decrease of the barrier properties upon incorporation of inhibitor filled nanocontainers (see Figure S2 in the Supporting Information).

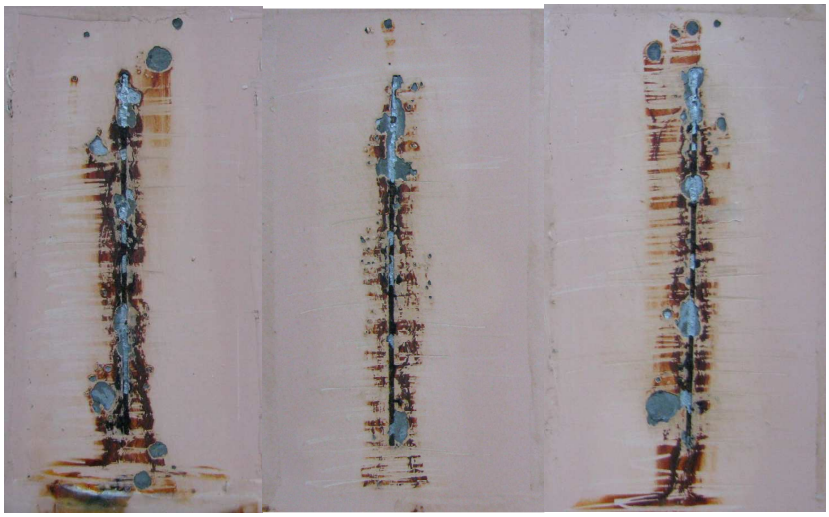

(A) (B) (C)

Figure 6. Neutral salt spray test results for polyepoxy coating without Zn phosphate in the presence of Korantin SMK loaded halloysite nanotubes with further deposition of PMA layer at 1 wt% (A, delamination distance 4.2 mm); 3 wt% (B, delamination distance 2.3 mm) and 5 wt% (C, delamination distance 3.4 mm) of nanocontainer concentration, 1000 hours of the test.

Figure 6 shows that the addition of the polyelectrolyte layer does not have sufficient improvements of the inhibitor-loaded nanocontainer-based coatings probably due to the interaction between polyelectrolyte shell and polyepoxy coating. However, the selection of the proper inhibitor for the metal substrate to be protected is also very important step in design of the nanocontainer-based autonomic corrosion protection coatings.

Changing of the encapsulated Korantin SMK to other corrosion inhibitors used in the paper did not result in significant improvement of the corrosion protection comparing with Korantin SMK loaded halloysite nanotubes. Corrosion protection for all three encapsulated inhibitors is similar to the corrosion protection of the standard polyepoxy coating containing 20 wt% of zinc phosphate, and encapsulated Korantin SMK showed the best results. This is very important achievement especially when one compares the quantity of the inhibiting pigment – 20 wt% of zinc phosphate, with the quantity of the inhibitors introduced into the coating in halloysite-encapsulated form – 1 wt% (5 wt% of halloysites with 20 wt% of the encapsulated inhibitor).

Conclusion.

We performed comparative analysis of the corrosion protection properties of standard polyepoxy coating containing 20 wt% of the zinc phosphate with the polyepoxy

coatings impregnated with 1 wt% corrosion inhibitor (Korantin SMK, Halox 520 or $(NH_4)_2TiF_6$) encapsulated into halloysite nanotubes by neutral salt spray test (Ascott CC450XP salt spray chamber, ISO 9227, 5 wt% NaCl, 35℃, 1 mm scribe, 500 h or 1000 h time). Despite 20-times decrease of the inhibitor content, introduction of the halloysite nanotubes with encapsulated inhibitor into polyepoxy coating demonstrated similar corrosion protection performance. The encapsulation of the corrosion inhibitor effectively isolate it from the coating matrix inside nanocontainers (halloysite nanotubes), where it stays in active, not-bounded form, and controls release of the inhibitor only into the damaged parts of the coating.

Acknowledgement.

DS acknowledges ERC Consolidator grant ENERCAPSULE for financial support.

DG is grateful for the financial support of the Federal Ministry of Economics and Energy (BMWi), Germany in the framework of "EXIST Transfer of Research" program (Project "SigmA" Nr. 03EFCBB028) and G8 initiative. We thank Matthias Schenderlein and Enrico Scherke for the help in experimental work.

Literature.

[1] D.G.Shchukin, H. Möhwald, Science 341 (2013) 1458-1459.

[2] S.R. White, N.R. Sottos, P.H. Geubelle, J.S. Moore, M.R. Kessler, S.R. Sriram, E.N. Brown, S. Viswanathan, Nature 409 (2001) 794-797.

[3] D. Fix, D.V. Andreeva, D.G. Shchukin, Y.M. Lvov, H. Möhwald, Adv. Funct. Mater. 19 (2009) 1720-1727.

[4] D.G. Shchukin, H. Möhwald, SMALL 3 (2007) 926-943.

[5] J. Tedim, M.L. Zheludkevich, A.C. Bastos, A.N. Salak, A.D. Lisenkov, M.G.S. Ferreira, Electrochimica Acta 117 (2014) 164-171.

[6] D. Borisova, M. Schenderlein, D.G. Shchukin, ACS Applied Materials and Interfaces 4 (2012) 2931-2939.

[7] R.S. Jadhav, D.G. Hundiwale, P.P. Mahulikar, J. Applied Polymer Science 119 (2011) 2911-2916.

[8] T. Szabo, J. Telegdi, L. Nyikos, Progress in Organic Coatings 84 (2015) 136-142.

[9] T. Siva, S. Sathiyanarayanan, Progress in Organic Coatings 82 (2015) 57-67.

[10] H. Shi, F. Liu, E.H. Han, J. Mater. Sci. & Technology 31 (2015) 512-516.

[11] M. Kopec, K. Szczepanowicz, G. Mordarski, K. Podgorna, R.P. Socha, P. Nowak, P. Warszynski, T. Hack, Progress in Organic Coatings 84 (2015) 97-106.

[12] J. Carneiro, A.F. Caetano, A. Kuznetsova, F. Maia, A.N. Salak, J. Tedim, N. Scharnagl, M.L. Zheludkevich, M.G.S. Ferreira, RSC Advances 5 (2015) 39916-39929.

[13] D.G. Shchukin, G.B. Sukhorukov, Advanced Materials 16 (2004) 671-682.

[14] S. Mehta, G. Kaur, K. Bhasin, Pharmaceutical Research 25 (2008) 227-236.

[15] K. Köhler, D.G. Shchukin, H. Möhwald, G.B. Sukhorukov, Journal Phys. Chem. B 109 (2005) 18250-18259.

[16] S.V. Lamaka, M. Taryba, M.F. Montemor, H.S. Isaacs, M.G.S. Ferreira, Electrochemistry Communications 13 (2011) 20-23.

[17] H. Wei, Y. Wang, J. Guo, N.Z. Shen, D. Jiang, X. Zhang, X. Yan, J. Zhu, Q. Wang, L. Shao, H. Lin, S. Wei, Z. Guo, J. Mater. Chem. A 3 (2015) 469-480.

[18] M.L. Zheludkevich, J. Tedim, M.G.S. Ferreira, Electrochimica Acta 82 (2012) 314-323.

[19] M.F. Montemor, Surface & Coatings Technology 258 (2014) 17-37.

[20] E. Abdullayev, V. Abbasov, A. Tursunbayeva, V. Portnov, H. Ibrahimov, G. Mukhtarova, Y. Lvov, ACS Applied Materials and Interfaces 5 (2013) 4464-4471.

[21] E. Abdullayev, Y. Lvov, J. Nanoscience Nanotechnology 11 (2011) 10007-10027.

[22] Y. Lvov, W. Wang, L. Zhang, R. Fakhrullin, Adv. Mater. 28 (2016) 1227-1250.

[23] E. Abdullayev, R. Price, D. Shchukin, Y. Lvov, ACS Applied Materials and Interfaces 1 (2009) 1437-1443.

[24] D.G. Shchukin, S.V. Lamaka, K.A. Yasakau, M.L. Zheludkevich, M.G.S. Ferreira, H. Mohwald, J. Phys. Chem. C 112 (2008) 958-964.

[25] M.L Zheludkevich, S.K. Poznyak, L.M. Rodrigues, D.Raps, T. Hack, L.F. Dick, T. Nunes, M.G.S. Ferreira, Corrosion Science 52 (2010) 602-611.

[26] D. Grigoriev, D. Akcakayiran, M. Schenderlein, and D. Shchukin, Corrosion 70 (2014) 446-463.

[27] O.Y. Weng, A. Takahara, Y.M. Lvov, J. of Amer. Chem. Soc. 134 (2012) 1853-1859.